JOURNAL OF GEOPHYSICAL RESEARCH, VOL. 85, NO. C9, PAGES 4957–4966, SEPTEMBER 20, 1980

Ocean Wave–Radar Modulation Transfer Functions From the West Coast Experiment

J. W. WRIGHT, W. J. PLANT, AND W. C. KELLER

Environmental Sciences Division, Naval Research Laboratory, Washington, D. C. 20375

W. L. JONES

NASA/Langley Research Center, Hampton, Virginia 23665

Short gravity-capillary waves, the equilibrium, or the steady state excitations of the ocean surface are modulated by longer ocean waves. These short waves are the predominant microwave scatterers on the ocean surface under many viewing conditions so that the modulation is readily measured with CW Doppler radar used as a two-scale wave probe. Modulation transfer functions (the ratio of the cross spectrum of the line-of-sight orbital speed and backscattered microwave power to the autospectrum of the line-of-sight orbital speed) were measured at 9.375 and 1.5 GHz (Bragg wavelengths of 2.3 and 13 cm) for winds up to 10 m/s and ocean wave periods from 2–18 s. The measurements were compared with the relaxation-time model; the principal result is that a source of modulation other than straining by the horizontal component of orbital speed, possibly the wave-induced airflow, is responsible for most of the modulation by waves of typical ocean wave period (10 s, say). The modulations are large; for unit coherence, spectra of radar images of deep-water waves should be proportional to the quotient of the slope spectra of the ocean waves by the ocean wave frequency.

1. MODULATION OF SHORT WAVE EQUILIBRIUMS

Short gravity-capillary waves, the equilibrium excitations of the ocean surface, are modulated by longer ocean waves. Generated by the wind, limited by wave-wave interactions and dissipation, affected by the fluxes of the air-sea boundary and the long waves, the steady state reached by these short waves still presents an intractable, theoretical problem. Modulation of the equilibrium can, nonetheless, be treated phenomenologically by expansion about the steady state (section 5) and be measured with the CW Doppler radar used as a two-scale wave probe [*Plant et al.*, 1978] (section 2). Thus the study of ocean wave–radar modulation transfer functions is an attractive means for examining the air-sea interface.

It is evident from our results (sections 2 and 3) that two-scale descriptions of the ocean surface are apt. Two-scale theories for microwave scattering from the ocean are reviewed by *Valenzuela* [1978]. The scatterers are the short waves; the successful assumption (first-order Bragg scattering) is that the local scattering cross section is proportional to the spectral intensity of the surface wave with wave vector in the plane of incidence (the plane containing the incident microwave vector and the local normal to the surface) and of magnitude $2k_0 \cos \theta$, where k_0 is the microwave number and θ the radar depression angle (Figure 1). At the winds we encountered (10 m/s and less) the microwaves we used (20 and 3.2 cm in wavelength) were sufficiently long that scattering associated with wave breaking was probably insignificant. Higher-order Bragg scattering is observed in wave tanks [*Valenzuela*, 1974; *Plant and Wright*, 1977; *Wright*, 1978], but scattering cross sections and, by inference, the short wave spectral intensities, are 3–10 dB larger in linear wind-wave channels than on the ocean. Compelling evidence of higher-order scattering is missing from previous measurements of microwave scattering from the ocean as well as from those reported here. Apparent anomalies (section 6) in our results become no more explicable if one assumes the occurrence of higher-order scattering (section 7).

A well known source of modulation of the short waves is straining [*Longuet-Higgins and Stewart*, 1964; *Phillips*, 1966] by the horizontal component of orbital speed of the long wave. A principal result of the present work is that modulations at the frequencies of typical ocean waves are largely due to some other source of modulation (section 6). The dependences of the modulation on modulating ocean wave frequency, and, partially, upon wind speed, are qualitatively consistent with wave-induced airflow as a modulator, but positive identification of the modulation source remains to be made.

Laboratory experiments [*Keller and Wright*, 1975] indicate that the response of wind-generated short waves to modulation is a relaxation. A value for the relaxation rate of 2.3 cm waves equal to about twice the growth rate was obtained by *Keller and Wright* [1975] by fitting laboratory results for modulation by 0.575 Hz waves to the relaxation model, assuming straining to be the sole source of modulation. We reanalyzed the laboratory data, assuming the presence of an additional source of modulation; the overall fit to the model is good, using a relaxation rate equal to the growth rate. This latter relationship between growth and relaxation rates is reasonable for the oceanic data as well.

2. MEASUREMENT OF MODULATION TRANSFER FUNCTIONS WITH CW DOPPLER RADAR

The principle of the measurement is described elsewhere [*Plant and Wright*, 1977]. Briefly, a microwave antenna (Figure 1) illuminates a portion of the ocean surface small in comparison with the wavelength of any modulating wave of interest. The short gravity-capillary waves, the predominant microwave scatterers, are advected about by the large wave. The Doppler shift caused by the line-of-sight component of the scatterer motion causes a frequency modulation of the co-

Paper number 80C0439.

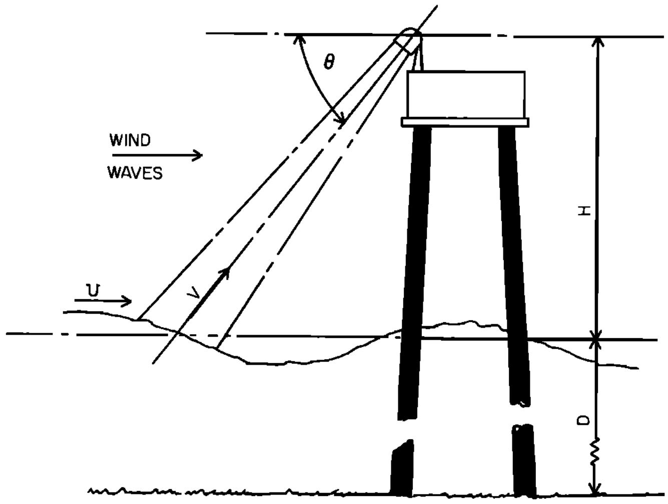

Fig. 1. Schematic diagram of a CW Doppler radar used as a two-scale wave probe.

herently received microwave signal; the amplitude modulation of the received signal is, essentially, the desired quantity. Let $P(t)$, the square of the homodyne detected [*King,* 1978] microwave voltage which, in turn, is proportional to the backscattered electromagnetic field, be called the instantaneously received power. Let $V(t)$ be the instantaneous line-of-sight speed obtained by frequency demodulation (frequency-to-voltage conversion) of the received signal. Then if G_{PV} is the cross spectrum of the instantaneously received power and instantaneous line-of-sight speed and G_{VV} is the autospectrum of the latter, define

$$m(\Omega) = \frac{C(\Omega)}{\bar{P}} \frac{G_{PV}(\Omega)}{G_{VV}(\Omega)} \tag{1}$$

The phase speed $C(\Omega)$ and mean received power $\bar{P}$ normalize the modulation transfer function, $m(\Omega)$, making it dimensionless; $G_{PV}(\Omega)$ is, of course, complex. To fix ideas, suppose the plane of incidence, the plane containing the microwave propagation vector, and the normal to the undistrubed ocean surface, also contain the direction of a monochromatic, modulating surface wave of frequency Ω and wave number K, propagating in water of depth D; the depression angle is θ. Then

$$V(t) = V_0 \cos(\Omega t + \phi_s) \tag{2}$$

$$\tan \phi_s = \tanh KD \tan \theta \tag{3}$$

$$V_0/U_0 = [\cos^2 \theta + \sin^2 \theta \tanh^2 KD]^{1/2} \tag{4}$$

and

$$P = \bar{P}\,[1 + m\,(Vo/C) \cos(\Omega t + \phi)] \tag{5}$$

where ϕ_s is the phase angle by which the line-of-sight speed leads the horizontal component of orbital speed, $U = U_0 \cos \Omega t$.

The site of the measurements was the Naval Oceanographic Systems Center tower, located in 18 m of water off Mission Beach, California. Two CW Doppler radars, transmitting at 1.5 and 9.375 GHz, were mounted 13 and 12 m, respectively, above mean sea level and were operated with vertical polarization (E vector in the plane of incidence) at a depression angle of 40°. The illuminated area was about 3 × 4 m at 1.5 GHz and 1.5 × 2 m at 9.375 GHz. Wave tank measurements [*Keller and Wright,* 1976] indicate that the measurement technique is viable when the wavelength of the modulating wave is as short as 6 times the length of the illuminated patch. This sets an upper limit on the frequency of the modulating wave of about 0.3 Hz for the 1.5 GHz system and about 0.5 Hz for the 9.375 GHz system.

The prevailing wind was onshore during the period of the experiment (February–March 1977); all the measurements reported here were made with the radars looking windward. The waves were usually broad-band swell systems; the line-of-sight orbital speed spectrum of Figure 2*a* is not atypical. The radars were visually aimed directly into the waves. This was not entirely possible for waves coming from south of west because of obstruction of the radar view by tower appurtenances, but reported cases are limited to those in which the difference between direction of dominant wave propagation and radar azimuth did not exceed 30°. The data include cases of long (up to 18 s period) underlying swell of small amplitude which nonetheless provided measurable modulations. We could not, of course, determine the direction of those low swells visually; we were, in fact, largely unaware of their presence at the time. As the radars were generally aimed within 10° or 20° of west, these low swells had likely been refracted into the direction of radar look, and the temptation to include these modulations at low frequencies was irresistible. Following our previous practice [*Plant et al.,* 1978] we excluded cases in which a difference of more than 40° existed between any pair of the three directions; wind direction, direction of travel of dominant wave, and radar azimuth.

Fully coherent data from the 1.5- and 9.375-GHz radars were recorded on an FM tape recorder synchronously with data from a vane anemometer mounted 5 m above the upper deck of the tower. Independent, wind-tunnel calibrations of the vane anemometer carried out before and after the experiment were in excellent agreement.

3. EXPERIMENTAL RESULTS

The coherent microwave records were frequency and amplitude demodulated as outlined in section 2, and the pairs of demodulated records were cross-correlated, using a Nicolet Scientific Instruments model 440 dual channel FFT analyzer. Records of 20 min duration were analyzed with a frequency resolution of 0.0125 Hz, but subsequent averaging over both frequency and multiple records, described hereinafter, strips these numbers of much of their statistical significance. The average value of the coherence was about 0.6 for correlations of 1.5 GHz data and about 0.5 for the 9.375-GHz data. Coherences as large as 0.8 were observed; modulation transfer functions corresponding to coherences less than 0.3 were excluded. This lower limit on the coherence insured that 95% confidence limits on transfer functions were less than 70% of the mean value, usually much less.

The phase and amplitude of the measured modulation transfer functions were further averaged over frequency bands centered on various frequencies f and having widths equal to 20% of f (no additional averaging was done for frequencies 0.075 Hz and less). Wind speed was averaged over the 20-min duration of individual records, records were classified into 1 m/s bands of average wind speed, and the modulation transfer functions for all records within each band were averaged. A few records in which the wind speed, the received power, or both, varied precipitously were excluded.

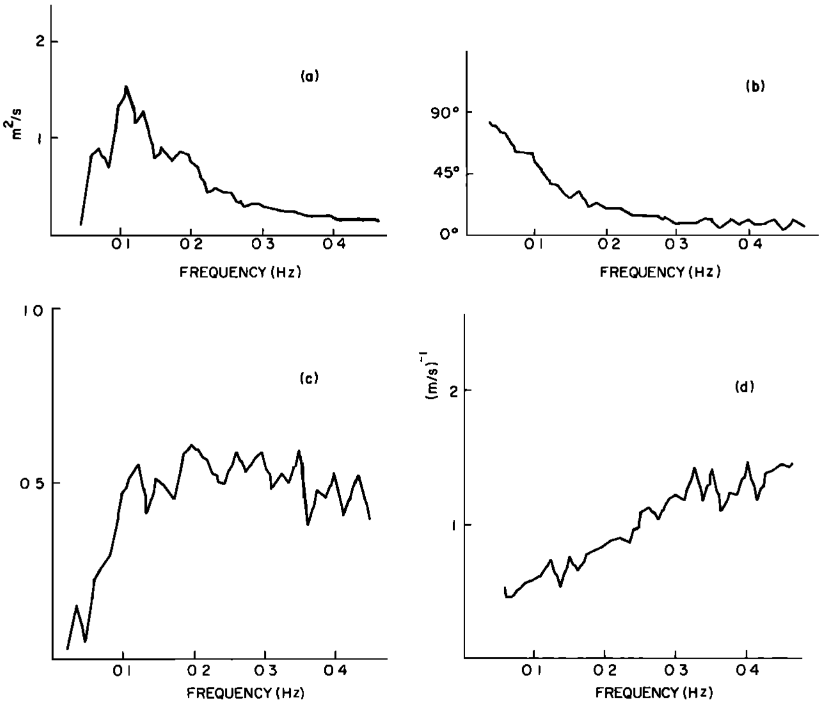

Fig. 2. Modulation spectra of the demodulated return of the 9.375 GHz radar. Wind speed = 7.5 m/s. (*a*) Line-of-sight component of orbital speed; (*b*) phase of the modulation transfer function; (*c*) coherence; (*d*) modulus of the modulation transfer function divided by the ocean wave phase speed, m/c.

The transfer functions shown in Figures 3 and 5 are referred to the line-of-sight velocity as defined by (1). The transfer function, referred to the horizontal component of orbital speed, a more useful quantity for interpretive purposes, is obtained by multiplying m by V_0/U_0 given by (4). Values calculated for the parameters of the West Coast Experiment are given in Table 1. However, the phases given in Figures 4 and 6 have been referred to the horizontal component of orbital speed, using the phase of the line-of-sight speed with respect to the horizontal orbital speed given by (3). Thus the origin of phase is the crest of a wave; positive phase is forward of the crest. Although the transfer functions, before averaging over the wind speed bands, exhibited scatter as large as a factor of 2, the fully averaged modulus (Figures 3 and 5) and phase (Figures 4 and 6) show smooth, stable dependences on modulating frequency and wind speed. Many of these data points are averaged over 10 or 15 records; the influence of other variables on the modulation transfer functions may have disappeared after averaging. We found no systematic dependence on the relative directions of wind, radar, and waves alluded to in section 2.

The distinctive feature of our previous measurements of modulation transfer functions from shoaling waves at 9.375 GHz [*Plant and Wright,* 1978] was the occurrence of a large peak at a wind speed of 5–6 m/s. The same phenomenon occurs in the present data but at a lower windspeed, 4–5 m/s (Figure 7*a*). In view of the present result that the transfer functions increase with decreasing frequency (Figures 3 and 5), we have replotted the earlier data from shoaling waves (Figure 7*b*), grouping it into the two frequency bands into which it naturally falls. Larger values of the transfer functions are observed at lower frequencies for the shoaling waves also. The water depth in the case of the earlier data (Figure 7*b*) was 3–4 m in comparison with 18 m at the Mission Beach site.

Modulation transfer functions at a fixed wind speed, plotted versus rms line-of-sight orbital speed (Figure 8) for some cases where the wave spectra were single peaked and otherwise simple, do not show any significant dependence on the orbital speed. The largest wave represented, however, was probably about 3 m peak to trough. Larger waves might exhibit nonlinear modulations, which have been observed in wave tank experiments [*Keller and Wright,* 1975].

4. MODULATION CAUSED BY TILTING AND RANGE VARIATION

The instantaneously received power is proportional to the product of the area illuminated by the antenna and the local scattering cross section per unit area σ_0. The scattering cross section has an inherent dependence on angle of radar incidence which, together with the dependence of the illuminated area on the same angle, results in a contribution to the modulation transfer function caused by wave slope which we denote by t. The contribution caused by the change in radar range as the illuminated area rides up and down the wave is denoted r. Because are dealing with modulating processes linear in the wave amplitude, we have

$$(V_0/U_0)m = m' - jt + r \tag{6}$$

where m' is the portion of the transfer function caused by the modulation of the amplitude of the small waves, and all transfer functions on the right-hand side of (6) are now referred to the horizontal component of orbital speed. In the case of first-order Bragg scattering from the small waves, the transfer function caused by tilt is found to be [*Keller and Wright,* 1975]

$$t = \left(\frac{1}{G}\frac{dG}{d\theta} - \tan\theta\,\frac{k}{F_0}\frac{\partial F_0}{\partial k}\right)\tanh KD \tag{7}$$

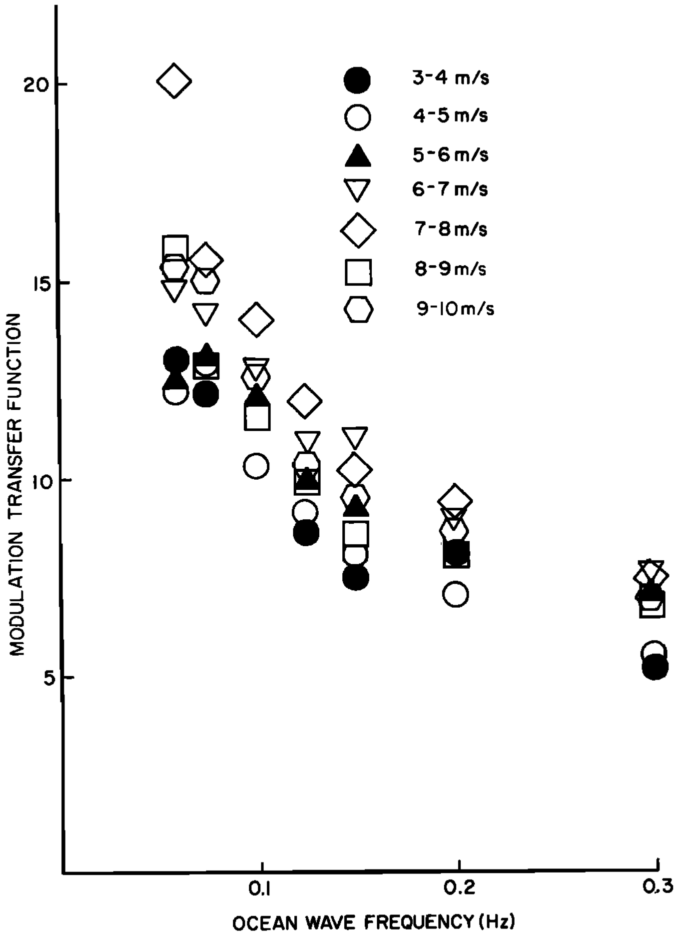

Fig. 3. Modulus of the 1.5-GHz (Bragg wavelength = 13 cm) transfer functions.

where θ is the depression angle, $F_0(k)$ is the mean surface displacement spectrum of the short waves, K is the wave number of the long wave, D is the water depth, and G is a first-order scattering function defined by *Keller and Wright* [1975].

The radar range at both microwave frequencies was about d^2/λ_0, where d is the antenna diameter and λ_0 is the microwavelength. Assuming this to be well enough into the far field that the illuminated area depends quadratically on range, we find

$$r = \frac{2 \tanh KD}{KH} \tag{8}$$

where H is the height of the antenna above the mean water level. The transfer functions caused by tilt and range change (Figure 9) computed from (7) and (8) are small in comparison with the measured functions (Figures 3 and 5) over most of the range of wind speed and ocean wave frequency considered here. Most of the modulation of the scattered power is due to the modulation of the amplitude of the short waves.

5. Relaxation of Gravity-Capillary Waves

The response of short, wind-generated waves to modulation has been explained as a relaxation [*Keller and Wright,* 1975]. The idea is that the short waves, if perturbed from equilibrium, will relax back at an exponential rate called the relaxation rate. The relaxation rate is a functional of the short wave spectrum; ultimately, it is determined by wave-wave and wind-wave interactions as well as dissipation. However, at present the theory is phenomenological, and the relaxation rate is an adjustable parameter. The reasons for choosing certain values for this, and other incompletely known parameters, become more perspicuous upon consideration of the relaxation of a pair of waves which simulate short gravity waves coupled to capillary waves by the second-order resonant interaction [*Valenzuela and Laing,* 1972; *Plant and Wright,* 1977; *Plant,* 1979].

Suppose, following *Keller and Wright* [1975], that a wind-generated short gravity-capillary wave equilibrium is perturbed by a much longer, modulating wave (as is in section 2) which we specify by the horizontal component of orbital speed, $U(x, t)$. The transport equation for the response of the wind-wave system, written for the action spectrum, $A \equiv \rho_w c^0(k)F(k)$ where $F(k)$ is the wave height spectrum, is

$$\frac{\partial A}{\partial t} + (c_g{}^0 + U)\frac{\partial A}{\partial x} - k\frac{dU}{dx}\frac{\partial A}{\partial k} = \beta A + H(A, u_*, k) \tag{9}$$

where c^0 and $c_g{}^0$ are the phase and group speeds, respectively, of the short wave in the absence of the long wave, β is the rate of energy input from the wind, and $H(A, u_*, k)$ is the interaction functional including dissipation. Denoting the gravity

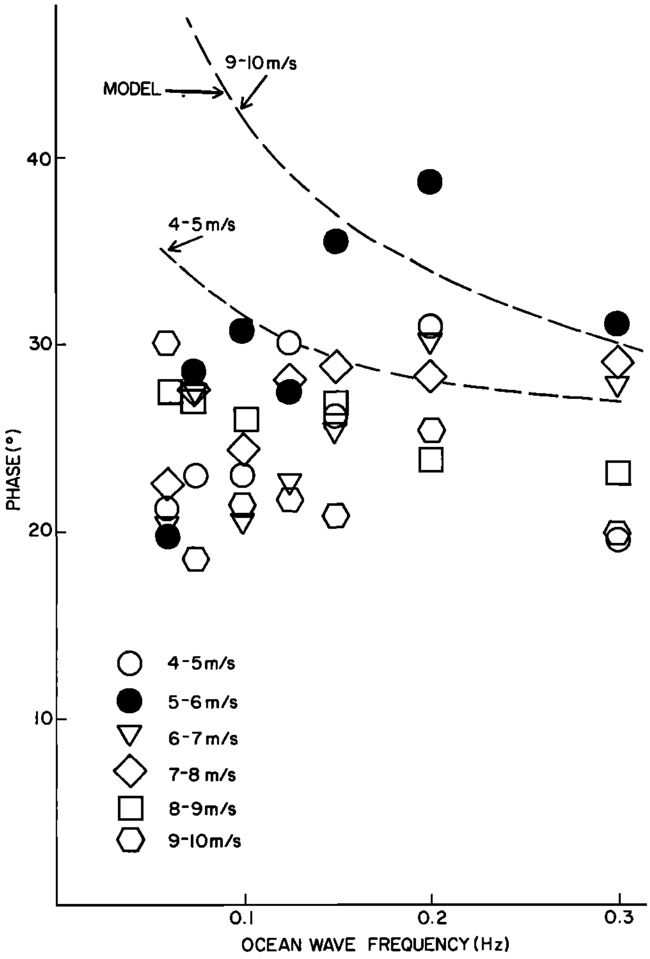

Fig. 4. Phase of the 1.5-GHz (Bragg wavelength = 13 cm) transfer functions. Phases are measured from wave crests and are positive leading the crest. Dashed lines are theoretical predictions assuming modulation caused solely by straining.

and capillary components of our pair of coupled waves by the subscripts g and c, respectively, we assume

$$H_g = -\alpha A_g A_c \tag{10a}$$

$$H_c = \alpha A_g A_c - \gamma A_c^2 \tag{10b}$$

where the parameters α and γ are to be determined from the equilibrium conditions.

Returning to (9), write

$$A = \bar{A} + a \tag{11}$$

with

$$\bar{a} = 0 \qquad \frac{\partial \bar{A}}{\partial t} = 0 \tag{12}$$

Taking the time average of (9) and assuming $\bar{U} = 0$ and $\partial \bar{A}/\partial x = 0$

$$\overline{U\frac{\partial a}{\partial x}} - k\overline{\frac{dU}{dx}\frac{\partial a}{\partial k}} = \overline{\beta A} + \bar{H} \tag{13}$$

Suppose $U(x, t)$ is a simple, progressive modulating wave

$$U = U_0 \exp\left[j(Kx - \Omega t)\right] \tag{14}$$

which elicits a periodic response from the wind-wave system. The equation for a, obtained by subtracting (13) from (9) may then be solved by expansion in a perturbation series in U_0/C. Adopting a vector notation for the gravity-capillary wave

$$\mathbf{A} = [A_g, A_c] \tag{15}$$

and neglecting the group speeds of the short wave in comparison with the phase speed of the long wave, we obtain, correct to second order in U_0/C

$$(j\Omega + \mathbf{J})\mathbf{a} = -\left(\frac{U_0}{C}\right)\bar{\mathbf{A}}\,\mathbf{S} \tag{16}$$

where

$$\mathbf{J} = \begin{pmatrix} \beta_g - \alpha\bar{A}_c & -\alpha\bar{A}_g \\ \alpha\bar{A}_c & \beta_c + \alpha\bar{A}_g - 2\gamma\bar{A}_c \end{pmatrix} \tag{17a}$$

and

$$\bar{\mathbf{A}} = \begin{pmatrix} A_g & 0 \\ 0 & A_c \end{pmatrix} \tag{17b}$$

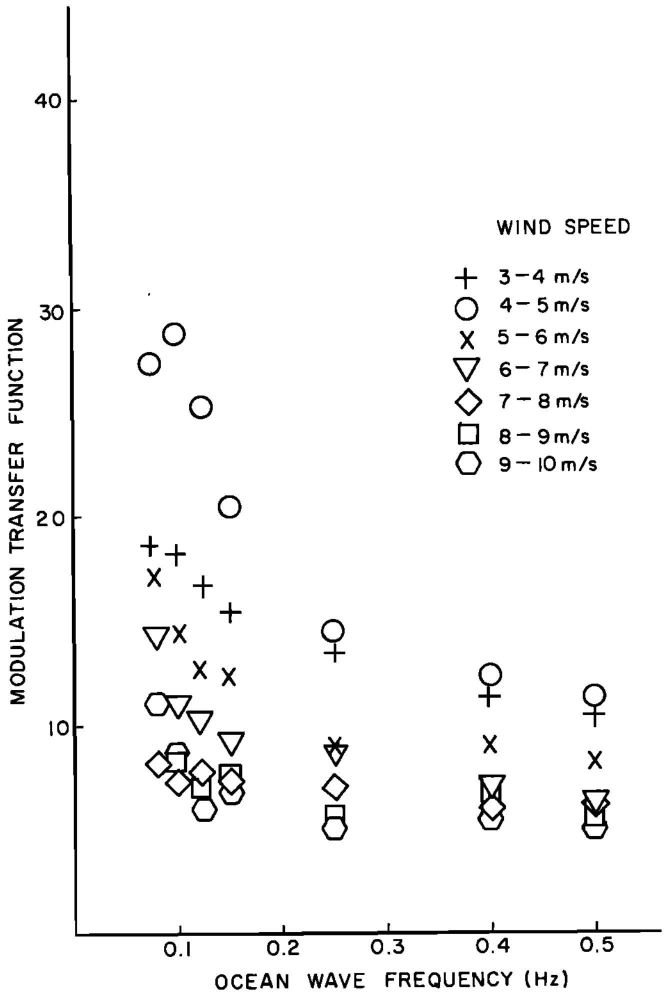

Fig. 5. Modulus of the 9.375-GHz (Bragg wavelength = 2.3 cm) transfer functions.

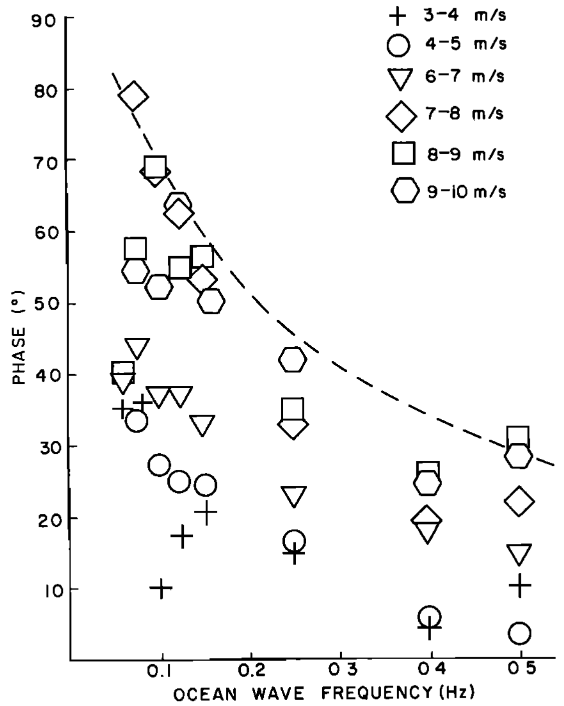

Fig. 6. Phase of the 9.375-GHz (Bragg wavelength = 2.3 cm) transfer functions. Phases are measured from wave crests and are positive leading the crest. Dashed line is a theoretical prediction assuming modulation caused only by straining.

TABLE 1. Ratio of Line-of-Sight Velocity to Horizontal Component of Orbital Velocity

f, Hz	λ, m	V_0/U_0, $\theta = 40°$
0.0220	600	0.775
0.0328	400	0.786
0.0433	300	0.800
0.0632	200	0.834
0.0712	175	0.849
0.0814	150	0.869
0.0947	125	0.894
0.1125	100	0.927
0.1316	80	0.955
0.1576	60	0.981
0.1968	40	0.997
0.2278	30	1.000

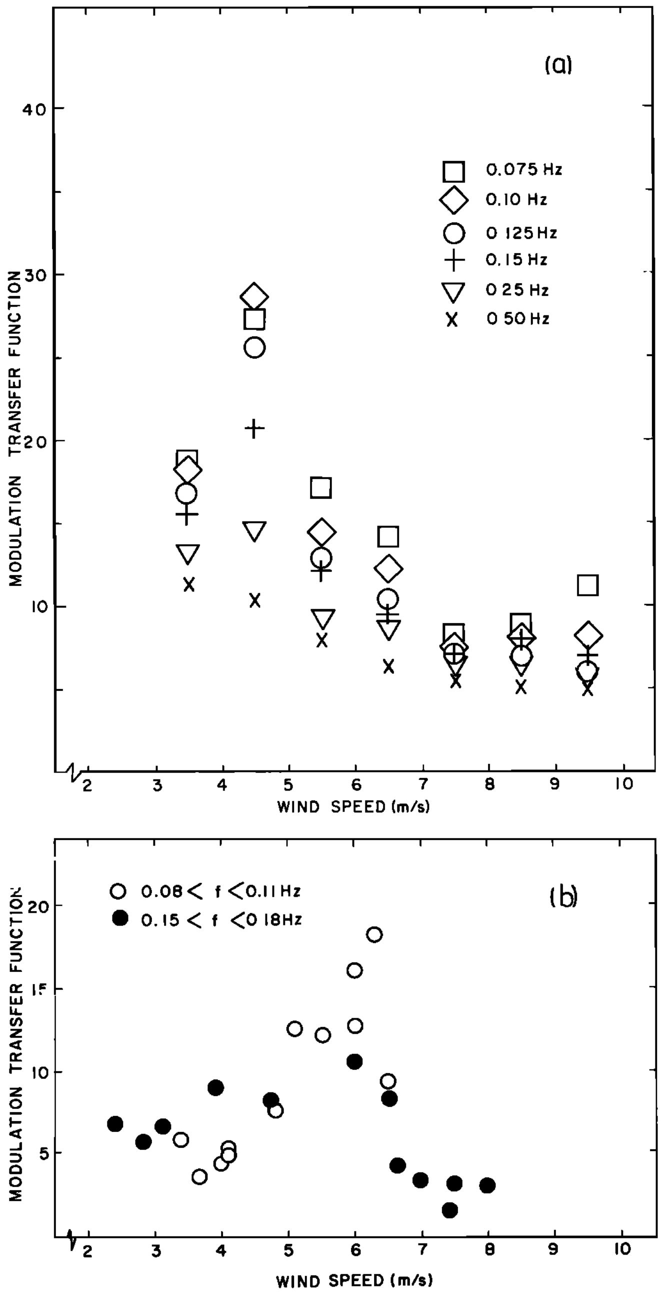

Fig. 7. Wind speed dependence of 9.375 GHz modulation transfer functions. (*a*) NOSC tower (this work); (*b*) Nags Head, North Carolina [*Plant et al.,* 1978].

The only source of modulation explicit in the development given above is $\mathbf{S}_s$, that owing to straining

$$\mathbf{S}_s = j\Omega\left[\frac{k}{\bar{A}_g}\frac{\partial \bar{A}_g}{\partial k} \quad \frac{k}{\bar{A}_c}\frac{\partial \bar{A}_c}{\partial k}\right] \tag{19}$$

but we allow for the inclusion of other modulation sources in (17*a, b*) by denoting the sum of all sources as $\mathbf{S} = (S_g, S_c)$. One additional source which comes to mind (it comes particularly readily to mind if it has been suggested, as it was to us, by Werner Alpers and Klaus Hasselmann) is the long wave-induced airflow.

The eigenvalues of J are the relaxation rates μ, that is,

$$\mathbf{J}\mathbf{a} = -\mu\mathbf{a} \tag{20}$$

The eigenvalues and eigenvectors are particularly perspicuous in the absence of the modulating wave. In that case the left-hand side of (13) vanishes and

$$0 = \beta_g\bar{A}_g - \alpha\bar{A}_c\bar{A}_g \tag{21a}$$

$$0 = \beta_c\bar{A}_c + \alpha\bar{A}_c\bar{A}_g - \gamma\bar{A}_c^2 \tag{21b}$$

The ratio $\bar{A}_g/\bar{A}_c$ is then

$$\bar{A}_g/\bar{A}_c = \frac{\gamma}{\alpha} - \frac{\beta_c}{\beta_g} \tag{22}$$

and this ratio is of the order of 10^3 for wind-generated waves in wave tanks. Because β_c/β_g does not exceed 10 [*Larson and Wright,* 1975; *Plant and Wright,* 1977], the ratio γ/α is of the order of 10^3 and the eigenvalues of (20) are

$$\mu_{1,2} \cong \beta_g \qquad (\gamma/\alpha)\beta_g \tag{23}$$

The corresponding eigenvectors can be taken as

$$e_{1,2} = (1, \alpha/\gamma) \qquad (1, 1) \tag{24}$$

The modes excited in response to perturbation of the steady state wind-wave system are thus a gravity-capillary wave in which the ratio of gravity to capillary wave amplitudes is the same as in the steady state and which relaxes back to the steady state at the growth rate of the short gravity wave component, and a capillary-like mode, composed of equal gravity and capillary components which relax at a rate large in comparison with the growth rate of the short gravity waves. The steady state response to modulation is a linear combination of these modes, but the capillary-like component contributes little because its relaxation rate is so large. The modulation transfer functions for the short gravity wave component is then

$$m' = -\frac{S_g}{j\Omega - \mu_1} \tag{25}$$

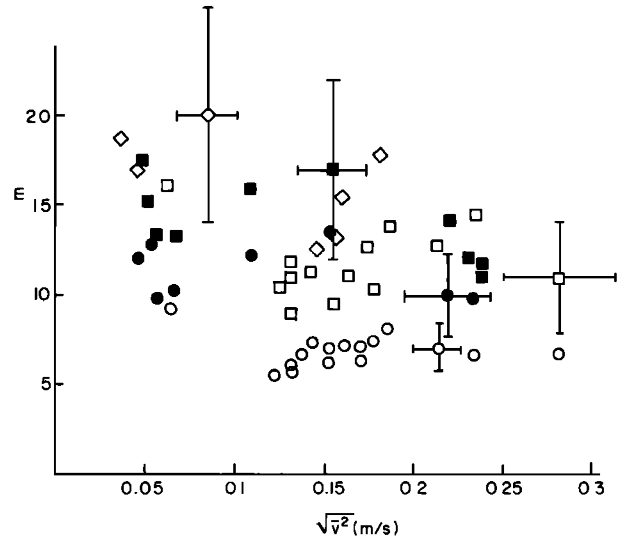

Fig. 8. Modulation transfer functions versus rms line-of-sight orbital speed at constant wind and constant ocean wave frequency. Solid points, 9.375 GHz; open points, 1.5 GHz. Solid square, 5–6 m/s, 0.1 Hz; solid dot, 5–6 m/s, 0.2 Hz; open square, 8–10 m/s, 0.1 Hz; open dot, 8–10 m/s, 0.3 Hz; open diamond, 7–8 m/s, 0.075 Hz.

or, if the only source of modulation is straining,

$$m' = \frac{-j\Omega[(k/F_0)(\partial F_0/\partial k) - \gamma_s]}{j\Omega - \beta_g} \tag{26}$$

where $\gamma_s \equiv (1 - c_g{}^0/c^0)$. The short gravity wave acts as though it were uncoupled to other waves in responding to modulation. The equality of relaxation rate and growth rate is the result of the assumption of quadratic dependence of the dissipation on the spectrum. Dependence on a higher power of the spectrum would have led to a larger multiple of the growth rate for the eigenvalue. More generally, $\bar{A}$ is determined by the mean action balance (13) so that it and the eigenvalues, which are functionals of $\bar{A}$, are amplitude dependent. These higher-order effects are discussed elsewhere by *Valenzuela and Wright,* [1979] but are not pursued here because the measured modulation transfer functions are independent of amplitude (Figure 8).

6. SOURCES OF MODULATION

Short wave growth rates increase fairly rapidly with increasing wind speed; if straining were the only source of modulation, the modulus of the transfer function would then decrease. The phase would be given by

$$\tan \phi = \beta/\Omega \tag{27}$$

so that the short waves would be found farther forward of the crests the greater the wind and the less the ocean wave frequency. This behavior is observed (Figures 5 and 6) in the 9.375 GHz (Bragg wavelength = 2.3 cm) data, but the waves are not as far forward as expected; according to (27), all the data points in Figure 6 should lie above and to the right of the dashed curve. The phase of the transfer function in the 1.5-GHz data (Bragg wavelength = 13 cm) does not conform to (27) at all being nearly independent of wind speed. The maximum transfer function caused by straining alone is $[-(k/F_0)(\partial F_0/\partial k) + \gamma_s]$; the values of transfer function of 15–30 shown in Figures 3, 5, and 7*a* are far larger than any values of $[-(k/F_0)(\partial F_0/\partial k) + \gamma_s]$ which have been reported. Finally, the increase in the modulus of the transfer functions with decreasing ocean wave frequency (Figures 3 and 5) is precisely counter to that expected from straining alone. If we wish to retain the relaxation model, we must admit other sources of modulation.

Thus if

$$S_g = j\Omega\left(\frac{k}{A_g}\frac{\partial \bar{A}_g}{\partial k}\right) + S_u \tag{28}$$

we have from (25)

$$m' = \frac{-[(k/F_0)(\partial F_0/\partial k) - \gamma_s] + jS_u/\Omega}{1 + j\beta/\Omega} \tag{29}$$

where S_u is an unidentified source of modulation. We calculated the phase and modulus of S_u from our data, assuming the relaxation rates to be equal to measured wave growth rates [*Larson and Wright,* 1975]. We let $-(k/F_0)\partial F_0/\partial k = 4$ for the 1.5 GHz (Bragg wavelength = 13 cm) data, but for the 2.3-cm waves we used spectra measured photometrically by *Wright and Keller* [1971]. These yield $-(k_0/F_0)\partial F_0/\partial k = 7.5$ at the lowest winds but decreasing to 4 at a windspeed of 8 m/s, and are qualitatively consistent with spectra derived from radar scattering cross sections of the ocean [*Wright,* 1968]. Values of γ_s were taken to be 0.4 for 13 cm waves and 0.1 for 2.3 cm.

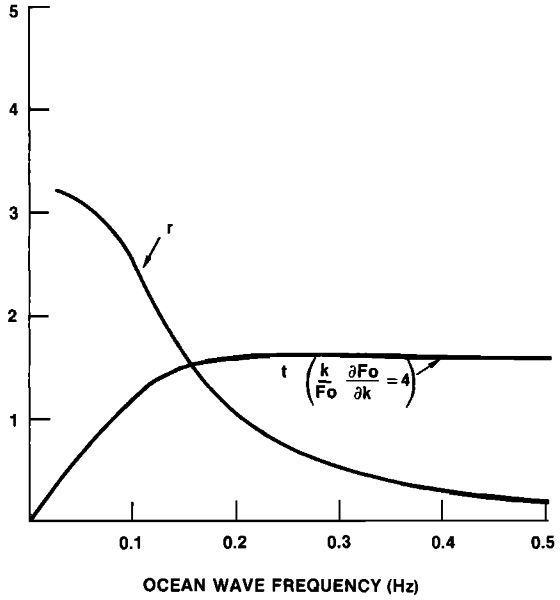

Fig. 9. Transfer functions owing to tilt t and range change r at NOSC tower. Depression angle = 40°, water depth = 18 m, antenna altitude = 13 m.

The source functions derived from 1.5 GHz data are relatively independent of ocean wave frequency (Figures 10*a* and 11*a*); those derived from 9.375 GHz (Figures 10*b* and 11*b*) are more scattered but do reflect the peak at a wind speed of 4–5 m/s evident in Figures 5 and 7. We reanalyzed the 9.375-GHz wave tank data of *Keller and Wright* [1975] letting the relaxation rate equal the growth rate; the calculated source (solid diamonds, Figures 10*b* and 11*b*) had about the same magnitude in the wave tank as on the ocean except that, curiously, no vestige of the pronounced peak appears in the wave tank data. The phases of all source functions except those for low frequencies in the 9.375 GHz data exhibit similar wind speed dependence, decreasing as wind speed increases. However, a large variation of phase at a constant wind speed was exhibited by the different sets of data.

In section 5 we noted the suggestion that wave-induced airflow might be a source of modulation. Wave growth rates are proportional to the square of the air-friction velocity (i.e., to the mean stress). One might expect a similar relation between the fluctuating stress caused by the wave-induced airflow and a fluctuating growth rate, more precisely

$$\frac{\Delta\beta}{\bar{\beta}} = \frac{\Delta\tau}{\bar{\tau}} \tag{30}$$

where $\Delta\beta$, $\Delta\tau$ and $\bar{\beta}$, $\bar{\tau}$ are the fluctuating and mean growth rates and stresses, respectively. A linearization, somewhat in the spirit of our relaxation model, was used to calculate the wave-induced airflow by *Townsend* [1972] who derived values of 2–5 times the growth rate for the quantity which becomes our S_u if the latter is indeed due to the wave-induced fluctuating stress, that is, if

$$(U_0/c)S_u = \Delta\beta \tag{31}$$

and (30) holds. We have plotted values of modulus and phase of S_u for a wave frequency 0.3 Hz obtained from Townsend's calculations in Figures 10 and 11 as solid lines. Moduli are not unacceptably different from those derived from our data, but

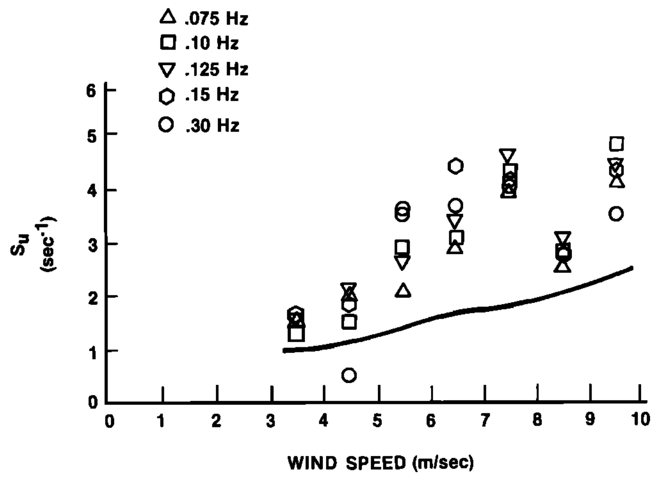

Fig. 10*a*

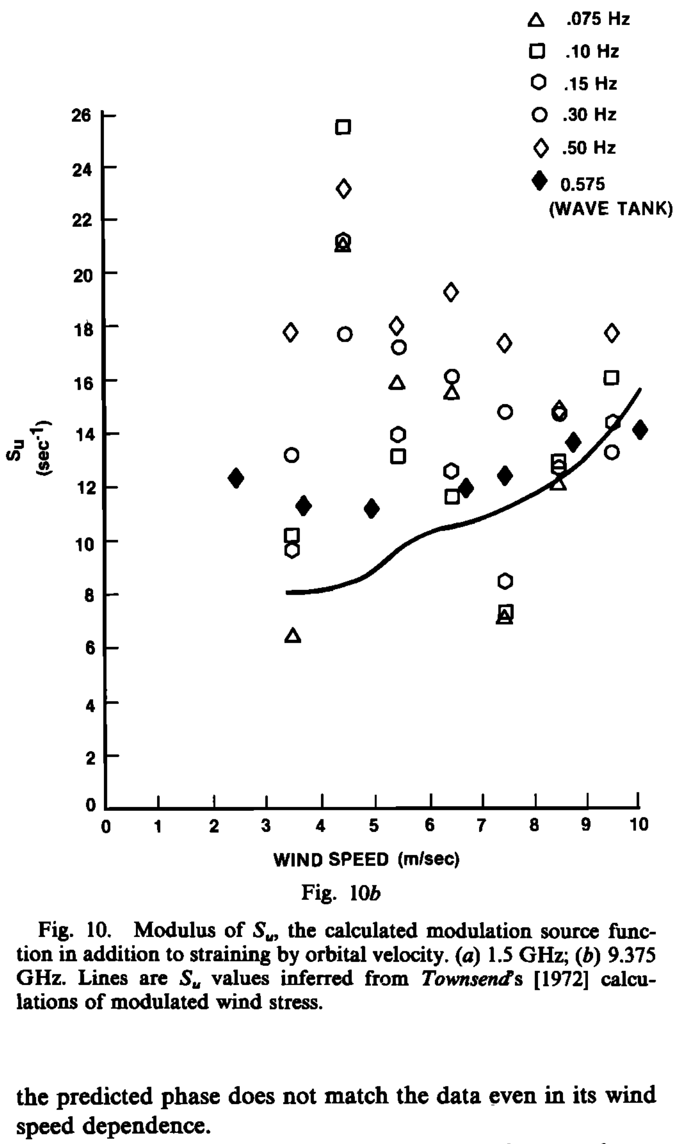

Fig. 10*b*

Fig. 10. Modulus of S_u, the calculated modulation source function in addition to straining by orbital velocity. (*a*) 1.5 GHz; (*b*) 9.375 GHz. Lines are S_u values inferred from *Townsend's* [1972] calculations of modulated wind stress.

the predicted phase does not match the data even in its wind speed dependence.

Townsend did not include variations in surface roughness (i.e., shorter waves) along his undulating surface. *Gent and Taylor* [1976] attempted to include this effect in their numerical calculations of air flow above water waves by letting the roughness length z_0 vary with position on the surface wave. They found that this variation had drastic effects on the surface stress even for small wave slopes. Both phases and magnitudes of $\Delta\tau$ depended critically on long-wave slope as well as the phase of the modulation of z_0 with respect to the wave. Source function phases obtained from this work for a wave of frequency 0.3 Hz and $U_0/C = 0.01$ are shown as dashed lines in Figure 11. Here z_0 has been assumed to have its maximum value leading the wave crest by 45°, a condition not atypical of the modulation of 2.3 and 13 cm waves. The wind speed dependence of the phase now shows better agreement with our data; inferred magnitudes of S_u are critically dependent on the depth of modulation of z_0, however.

7. Potpourri

All of the measurements reported here were made with vertically polarized microwaves which were chosen to make the measurement of wave slopes perpendicular to the plane of incidence unnecessary (the scattering is then insensitive to them). Horizontally polarized radiation used (e.g., in the SeaSat A synthetic aperture radar) would result in a stronger tilt dependence. Thus if the extra modulation (Figure 10*a*) increases with wind speed at winds larger than those encountered here, the transfer function applicable to SeaSat A imagery should remain large and relatively wind speed independent. The synthetic aperture radar wave image spectrum, properly calibrated, is G_{PP} (section 2)

$$G_{PP}(\Omega) = (P^2 m'^2 G_{VV}(\Omega))/(C^2\gamma(\Omega)) \tag{32}$$

for deep-water waves, $G_{VV}/C^2 \sim S(\Omega)$, the wave slope spectrum; a power law fit to the measured values of m for the 1.5-GHz data gives $m \sim \Omega^{-1/2}$. Hence if the coherence is independent of Ω

$$G_{PP}(\Omega) \sim \Omega^{-1}S(\Omega) \tag{33}$$

We remark that the SeaSat A SAR imagery is likely to be affected by scatterer motion [*Larson et al.*, 1976; *Elachi and Brown*, 1977] an effect not included in the modulation transfer functions given here.

This result for $G_{PP}(\Omega)$ also may be applied to the output of a dual frequency microwave scatterometer. *Plant* [1977] and *Alpers and Hasselman* [1978] have shown that the output of such a system may be written

$$E(\omega) = \int P(\omega')P(\omega - \omega')\,d\omega' + G_{PP}(2\Delta k \cos\theta, 0, \omega)/A \tag{34}$$

where $P(\omega)$ is the Doppler spectrum of the backscattered signal averaged over the illuminated area, $G_{PP}(\mathbf{k}, \omega)$ is the spectral density of backscattered power at $\mathbf{k}$ and ω, A is the area of the footprint, and ensemble averaging is implied. If a dispersion relation exists between ω and k, the integral of $E(\omega)$ over ω is

$$E = P^2 + G_{PP}(\Omega)C_g(\Omega)\psi(0)g/\Omega^2 A \tag{35}$$

where $\psi(0)$ is the angular part of G_{PP}, g is the gravitational acceleration, and Ω is the angular frequency corresponding to the wave number $2\Delta k \cos\theta$. Because $C_g \sim \Omega^{-1}$, the dual-frequency Bragg peak will go as $\Omega^{-4}S(\Omega)$ if the coherence is independent of Ω and $m \sim \Omega^{-1/2}$.

The growth rate of ocean waves caused by modulated stress was calculated by *Valenzuela and Wright* [1976] who assumed the short wave modulation to be entirely due to straining. The measured modulation is much larger; the long wave growth rate could be 2–3 times larger than they estimated. The trans-

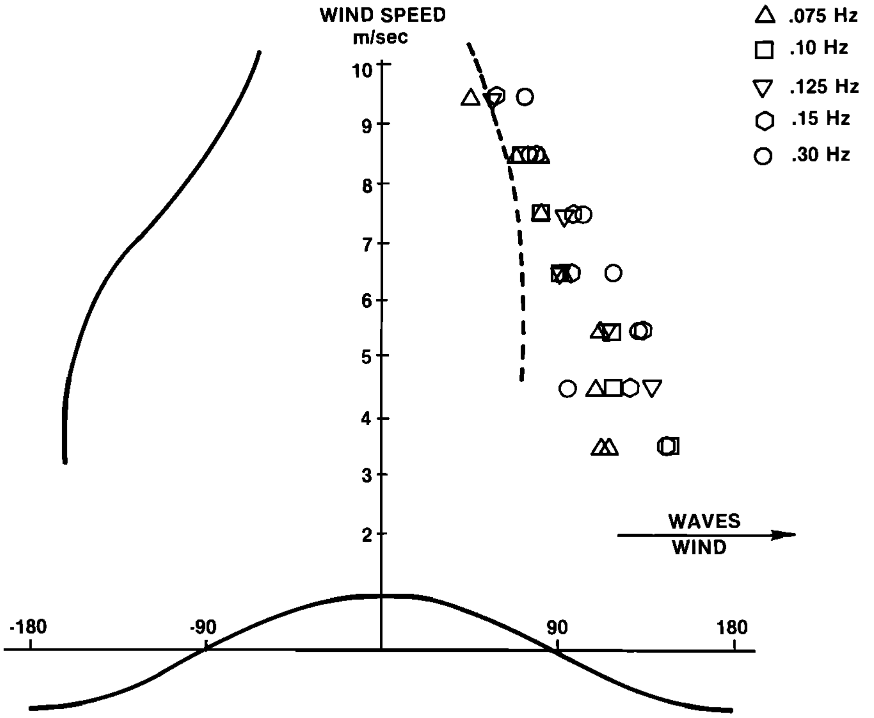

Fig. 11*a*

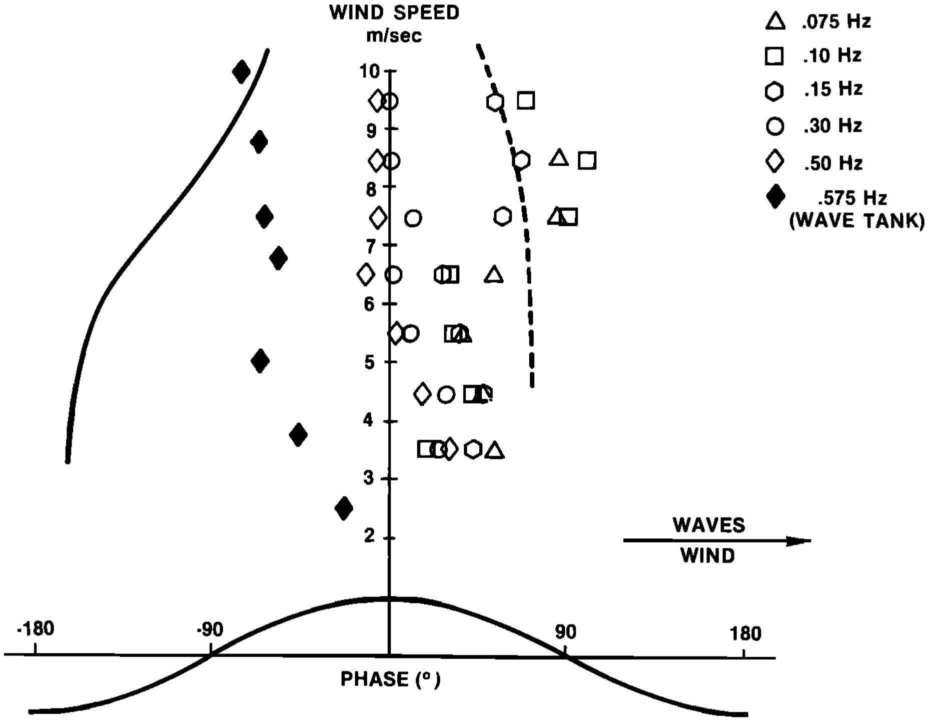

Fig. 11*b*

Fig. 11. Phase of S_ω, the calculated modulation source function in addition to straining by orbital velocity. (*a*) 1.5 GHz; (*b*) 9.375 GHz. Solid lines are phases inferred from *Townsend's* [1972] calculations of modulated wind stress. Dashed lines are phases obtained from *Gent and Taylor's* [1976] calculations of modulated wind stress, assuming a variable roughness length.

fer function for waves of typical dominant wave period (10 s, say) are so large that modulations could reach 100%, and become nonlinear, in fully developed seas. They would then provide a momentum flux to the long waves approaching the maximum possible value, estimated [*Garret and Smith,* 1976] to be $\tau_\omega \bar{s}$ where τ_ω is the mean wind stress and $\bar{s}$ is the rms slope of the long waves. The actual momentum flux in the Jonswap experiments was 5–20% of the wind stress [*Hasselmann et al.,* 1973] but the period of the dominant wave in those measurements was only about 5 s.

The marked difference between the wind speed dependences of the 1.5-GHz and 9.375-GHz transfer functions are pertinent to the persistent question of the influence of higher-order Bragg scattering. For wave systems with spectra which fall off rapidly with increasing wave number, this implies scattering from waves larger and longer than the Bragg wave; we would then expect to find, in the 9.375-GHz scattering, strong traces of the behavior of the 1.5-GHz scattering. These are not evident in the transfer functions. The principal anomaly in the behavior of the transfer functions, the peak in the 9.375-GHz data, is not plausibly explained by dependence of the relaxation rate on short wave number. Likewise, both 2.3 and 13 cm waves are generated by the same mechanism, instability of the viscous boundary layer [*Miles*, 1962; *Valenzuela*, 1976]; one would expect the source functions S_u for the two short waves to be similar if the source were indeed the wave-induced flow. Both the response of the short wind-generated waves to modulation and the modulation of short waves on the ocean need further study.

8. ENVOI

If the response of short gravity-capillary waves to modulation by ocean waves of typical period (10 s, say) is a relaxation, the modulation is largely due to a source substantially stronger than the straining of the short waves by the horizontal component of orbital speed of the long waves, possibly the wave-induced airflow.

Acknowledgments. The authors would like to thank R. Denton for his many contributions to the spectral analysis. We also are grateful to A. Cross for his efforts in constructing and installing the L-band system.

REFERENCES

Alpers, W., and K. Hasselmann, The two-frequency microwave technique for measuring ocean-wave spectra from an airplane or satellite, *Boundary Layer Meteorol., 13,* 215–230, 1978.

Elachi, C., and W. Brown, Models of radar imaging of ocean surface waves, *IEEE Trans. Antennas Propagat., AP-25,* 84–95, 1977.

Garrett, C., and J. Smith, On the interaction between long and short surface waves, *J. Phys. Oceanogr. 6,* 925–930, 1976.

Gent, P. R., and P. A. Taylor, A numerical model of the air flow above water waves, *J. Fluid Mech., 77,* 195–128, 1976.

Hasselmann, K., T. P. Barnett, E. Bouws, H. Carlson, D. E. Cartwright, K. Enke, J. A. Ewing, H. Gienapp, D. E. Hasselmann, P. Kruseman, A. Meerburg, P. Müller, D. J. Olbers, K. Richter, W. Sell, and H. Walden, Measurements of wind-wave growth and swell decay during the Joint North Sea Wave Project (JONSWAP), *Deut. Hydrogr. Z., 12, suppl. A,* 1–95, 1973.

King, R. J., *Microwave Homodyne Systems,* 367 pp., Peter Peregrinus, Stevenage, Herts, England, 1978.

Keller, W. C., and J. W. Wright, Microwave scattering and the straining of wind-generated waves, *Radio Sci., 10,* 139–147, 1975.

Keller, W. C., and J. W. Wright, Modulation of microwave backscatter by gravity waves in a wave tank, *NRL Rep. 7968,* Naval Res. Lab., Washington, D. C., 1976.

Larson, T. R., and J. W. Wright, Wind-generated gravity-capillary waves: Laboratory measurements of temporal growth rates using microwave backscatter, *J. Fluid. Mech., 70,* 417–436, 1975.

Larson, T. R., L. I. Moskowitz, and J. W. Wright, A note on SAR imagery of the ocean, *IEEE Trans. Antennas Propagat., AP-24,* 393–394, 1976.

Longuet-Higgins, M. S., and R. W. Stewart, Radiation stresses in water waves: A physical discussion with applications, *Deep Sea Res., 11,* 527–562, 1964.

Miles, J. W., On the generation of surface waves by shear flows, 4, *J. Fluid. Mech., 13,* 433–448, 1962.

Phillips, O. M., *The Dynamics of the Upper Ocean,* pp. 56–63, Cambridge University Press, New York, 1966.

Plant, W. J., Studies of backscattered sea return with a CW, dual-frequency, X-band radar, *IEEE Trans. Antennas Propagat., AP 25,* 28–36, 1977.

Plant, W. J., The gravity-capillary wave interaction applied to wind-generated, short-gravity waves, *NRL Rep. 8289,* Naval Res. Lab., Washington, D. C., 1979.

Plant, W. J., and J. W. Wright, Growth and equilibrium of short gravity waves in a wind-wave tank, *J. Fluid Mech., 82,* 767–793, 1977.

Plant, W. J., W. C. Keller, and J. W. Wright, Modulation of coherent microwave backscatter by shoaling waves, *J. Geophys. Res., 83,* 1347–1352, 1978.

Townsend, A. A., Flow in a deep turbulent boundary layer over a surface distorted by water waves, *J. Fluid Mech., 55,* 719–735, 1972.

Valenzuela, G. R., The effect of capillarity and resonant interactions on the second-order Doppler spectrum of sea echo, *J. Geophys. Res., 79,* 5031–5037, 1974.

Valenzuela, G. R., The growth of gravity-capillary waves in a coupled shear flow, *J. Fluid Mech., 76,* 229–250, 1976.

Valenzuela, G. R., Theories for the interaction of electromagnetic and oceanic waves—A review, *Boundary Layer Meteorol., 13,* 61–85, 1978.

Valenzuela, G. R., and J. W. Wright, The growth of waves by modulated wind stress, *J. Geophys. Res., 81,* 5795–5796, 1976.

Valenzuela, G. R., and J. W. Wright, Modulation of short gravity-capillary waves by longer-scale periodic flows—A higher order theory, *Radio Sci., 14,* 1099–1110, 1979.

Valenzuela, G. R., and M. B. Laing, Non-linear energy transfer in gravity-capillary wave spectra with applications, *J. Fluid Mech., 54,* 507–520, 1972.

Wright, J. W., A new model for sea clutter, *IEEE Trans. Antennas Propagat., AP-16,* 217–223, 1968.

Wright, J. W., Detection of ocean waves by microwave radar: The modulation of short gravity-capillary waves, *Boundary Layer Meteorol., 13,* 87–105, 1978.

Wright, J. W., and W. C. Keller, Doppler spectra in microwave scattering from wind waves, *Phys. Fluids, 14,* 466–474, 1971.

(Received June 21, 1979;
March 25, 1980;
March 30, 1980.)